

Laminate composites behavior under quasi-static and high velocity perforation

E. Mehrabani Yeganeh¹, G.H. Liaghat¹ and M.H. Pol^{*2}

¹ Department of Mechanical Engineering, Tarbiat Modares University, Tehran, Iran

² Department of Mechanical Engineering, Tafresh University, Tafresh, Iran

(Received July 31, 2016, Revised October 26, 2016, Accepted October 28, 2016)

Abstract. In this paper, the behavior of woven E-glass fabric composite laminate was experimentally investigated under quasi-static indentation and high velocity impact by flat-ended, hemispherical, conical (cone angle of 37° and 90°) and ogival (CRH of 1.5 and 2.5) cylindrical perforators. Moreover, the results are compared in order to explore the possibility of extending quasi-static indentation test results to high velocity impact test results in different characteristics such as perforation mechanisms, performance of perforators, energy absorption, friction force, etc. The effects of perforator nose shape, nose length and nose-shank connection shapes were investigated. The results showed that the quasi-static indentation test has a great ability to predict the high velocity impact behavior of the composite laminates especially in several characteristics such as perforation mechanisms, perforator performance. In both experiments, the highest performance occurs for 2.5 CRH projectile and the lowest is related to blunt projectiles. The results show that sharp perforators indicate lower values of dynamic enhancement factor and the flat-ended perforator represents the maximum dynamic enhancement factor among other perforators. Moreover, damage propagation far more occurred in high velocity impact tests than quasi-static tests. The highest damage area is mostly observed in ballistic limit of each projectile which projectile deviation strongly increases this area.

Keywords: static perforation; dynamic perforation; projectile nose shape; woven fabric composite laminate; energy absorption

1. Introduction

Fiber reinforced polymer (FRP) composites have been widely used in high performance applications because of their high specific strength and stiffness. The weight saving benefit of these composites has made them a suitable choice for aerospace, defense, marine and automotive uses. A disadvantage of FRP composite laminates is their low strength under transvers loadings such as localized static or impact loadings, which may extensively occur during their operation. Therefore, understanding the behavior of FRPs under perforation of lateral static or impact loadings is a significant concern for designers (Iremonger and Went 1996, Wen *et al.* 1997, Pol *et al.* 2013).

Great advantages of woven fiber composites, such as a better impact resistance or lower delamination area than unidirectional composites, have made them a widespread choice for aerospace or defense applications. Perforation behavior of composite structures is affected by

*Corresponding author, Assistant Professor, E-mail: m_h_pol@tafreshu.ac.ir

several exterior and interior factors. Perforator geometry is a very significant factor in perforation of composite plates. Valuable studies have been performed to investigate the effects of this factor on FRP composite plates (Ulven *et al.* 2003, Mines *et al.* 1999). In these studies, the common perforator shapes have been blunt, hemispherical and conical and have been frequently focused on high velocity impact. However, this kind of damage can occur by different perforator shapes and impact velocities.

Different shapes and velocities cause different damage mechanisms in composite structures. Iremonger and Went (1996) studied the penetration of different fragment simulating projectiles (FSPs) into EVA (ethylene vinyl acetate) laminate composites. They showed that the shear plugs are cut along projectiles right angled edges while their oblique faces cause tensile failure of fibers.

Wen *et al.* (1997) carried out penetration and perforation tests on laminate composites and sandwich panels using flat-ended, hemispherical and conical nosed perforators. These perforators were also experimentally investigated by Mines *et al.* (1999) for woven glass/polyester laminate composites. They concluded that the flat ended projectile has the largest dynamic enhancement factor, i.e. the ratio of impact perforation energy to static perforation energy, whilst this factor has the minimum values for conical and hemispherical ended missiles.

Gama and Gillespie (2008) modeled the ballistic penetration and damage mechanisms under conditions similar to quasi-static experiment. In this study, failure mechanisms, penetration and absorbed energy in the thick composites were investigated with both ballistic and quasi-static tests separately. They observed that the failure mechanism on ballistic impact test can be similar to the one in quasi-static experiments applying several boundary conditions (different spans). They obtained a developed quasi-static model to model the ballistic penetration and the absorbed energy in ballistic failure mechanism.

Yahaya *et al.* (2014) investigated quasi-static penetration and ballistic properties of non-woven kenaf fibres/Kevlar epoxy hybrid laminates and kenaf/epoxy and Kevlar/epoxy composites with different thicknesses. They concluded that the maximum force to initiate the penetration is higher in hybrid composites compared to kenaf/epoxy and Kevlar/epoxy composites. Hybridization of kenaf-Kevlar resulted in a positive effect in terms of energy absorbed (penetration) and maximum load. Moreover, in the case of ballistic tests, hybrid composites recorded lower ballistic limit and energy absorption than the Kevlar/epoxy composite.

The influence of projectile shape on carbon/epoxy laminate composites under high velocity impact was studied by Ulven *et al.* (2003). Conical projectile resulted in the greatest amount of energy absorption at ballistic limit followed by flat, hemispherical, and FSP (fragment simulating projectile), respectively. Projectile shape induced different failure mechanisms which resulted in different ballistic limits. They also showed that thin composite panels bend easily during a ballistic impact event and so a majority of projectile energy is absorbed, regardless of projectile shape.

Jordan and Naito (2014) studied experimentally the influence of fragment nose shapes on penetrating glass Phenolic. They found that the fragments with the sharper nose shapes were the most efficient penetrators.

Muhi *et al.* (2009) investigated the effect of Kevlar layer hybridization on the GFRP behavior under high velocity impact using flat-ended, hemispherical and conical projectiles. They found that hybridization improves the laminates performance under dynamic penetration. Their results also indicated that the flat-ended projectile shows the highest increase of absorbed energy due to hybridization.

The effects of several factors such as projectile geometry on penetration into Kevlar fabrics were experimentally verified by Khodadadi *et al.* (2013). They used flat-ended and hemispherical

projectiles in high velocity experiments and showed that both of projectiles cause tensile stress in fibers, but the sharp edges of flat-ended projectile create shear stress in fibers, too. Lower ballistic limit was exhibited by flat-ended projectile.

The effect of impactor shape on the low velocity impact response of thin woven carbon/epoxy laminate composites was investigated by Mitrevski *et al.* (2005) using a drop weight test rig with hemispherical, ogival and conical impactors. They found that the energy absorbed by the specimen is the highest for the conical impactor. The hemispherical impactor produced the highest peak force and lowest contact duration. Similar study on preloaded composite was performed by Mitrevski *et al.* (2006). The contact duration and deflection were found to decrease with increasing preload due to the stiffening caused by biaxial tension. The peak force, absorbed energy and damage area were largely unaffected by the preload.

In an experimental work, Icten *et al.* (2013) investigated the effects of impactor diameter on low velocity impact response of woven glass/epoxy laminate composites. They showed that the stiffness value increases with increasing impactor diameter. For low impact energies the absorbed energy decreased with increasing the diameter.

Indentation is a suitable test to evaluate the resistance of material against transverse damage. Baucom and Zikry (2003) discussed that indentation test data can be used to model and predict the material behavior in high velocity perforation. Impact damage mechanisms of laminate composites have also been similar to damage exhibited in indentation test (Xiao *et al.* 2007). Lee *et al.* (2003) investigated the indentation damage characteristics of hybrid carbon epoxy composites, under quasi-static contact loading of a hemispherical indenter.

Experimental and numerical investigation of shear punch dimensions on the compression behavior of glass/epoxy composites was studied by Manzella *et al.* (2011). They showed that fracturing through the fiber material occur at a characteristic angle irrespective of punch dimensions.

In present study, the behavior of glass/epoxy laminate composite in quasi-static indentation and high velocity impact tests was investigated using blunt, hemispherical, conical and ogival perforators. Two conical nose perforators with different cone angles and two ogival perforators with different caliber radius head were used to study the effects of perforator nose shape, nose length and the joining shape of projectile nose to its shank. Moreover, the results are compared in order to explore the possibility of extending quasi-static indentation test results to high velocity impact test results in different characteristics such as perforation mechanisms, performance of perforators, energy absorption, friction force, etc.

2. Experimental

2.1 Specimen manufacture

In this study, a glass/epoxy laminate composite was used as the target. The reinforcement was 2D woven E-glass fabric with an areal density of 200 g/m² with equal longitudinal and transverse mechanical properties. The polymeric matrix is a two parts epoxy. The base epoxy matrix is a diglycidyl ether of bisphenol A (DGEBA) named Epon 828 manufactured by Shell chemical company. The hardener curing agent is Jeffamine D-400 Polyoxypropylene diamine with molecular weight of 400 g/mol manufactured by Huntsman Corporation. According to the company recommendation, the mixing ratio of hardener to matrix is 55:100. 18 layered composite

panels with fiber volume fraction of 45% were manufactured using hand lay-up method. The laminate composites were cured by autoclave at temperature of 80°C and pressure of 2.5 bar for 150 minutes post-cured at temperature of 120°C and pressure of 1.5 bar for 150 minutes. The final thickness of composite laminates was 4.2 mm. The panel was cut into square plates with the dimension of 12×12 cm². A fixture with square unsupported span of 10×10 cm² and thickness 20 mm was used to clamp the specimen using 8 bolts. Fig. 1 shows the fixture used to clamp the composite targets for both impact and indentation tests.

Six types of projectile with different nose shapes were used to consider the effect of cylindrical perforator geometry on perforation of laminated composite. As Fig. 2 shows, the perforator nose geometries were flat-ended, hemispherical, conical with cone angle of 37°, conical with cone angle of 90°, ogival with caliber radius head (CRH) of 1.5 and ogival with caliber radius head of 2.5. Caliber radius head is the ratio of the perforator nose radius to its diameter. The caliber radius head is zero for flat-ended nose and 0.5 for hemispherical nose. The projectiles and indenters were all made of cold work tool steel with 10 mm diameter. All of the impact test projectiles were manufactured with equal mass of 9.3 g.

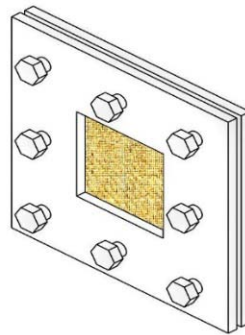


Fig. 1 Fixture used in indentation and high velocity impact tests

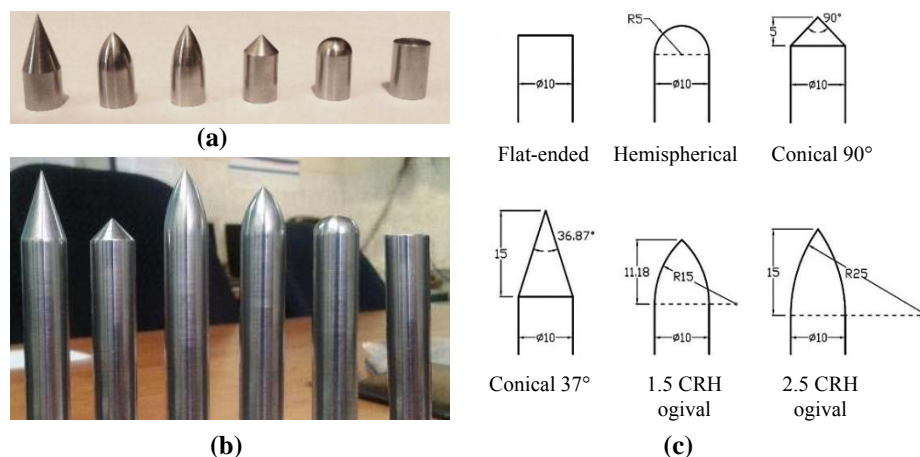


Fig. 2 (a) Perforators; (b) impact projectiles; (c) indenters; (d) geometry of perforators (All dimensions in mm)



Fig. 3 Gas gun set up

2.2 Ballistic test

The high velocity impact tests were carried out using gas gun test set up in Tarbiat Modares University (Fig. 3). The gas gun set up consists of a gas reservoir which is filled with air. The fast valve releases the pressure behind the projectile, causing it moves and reaches a constant speed along the 6 m barrel. The projectile initial velocity is measured by two separate lasers before striking the target. When the projectile passes the target, some deviation occurs which makes impossible to use two lasers to measure the residual velocity. So for this purpose, two separate rows of lasers (40 horizontal and 40 vertical lasers) were used.

Besides using different nose shapes, projectiles were fired with different initial velocity above the minimum velocity required for perforation in the sample (ballistic limit) to investigate the effects of initial velocity on the ballistic performance of different projectiles in the range of 120-180 m/s. For each projectile the first test was performed at high initial velocity to ensure full perforation.

In addition to the initial velocity and residual velocity, the damage area of laminate composite is measured too. According to Sutherland and Soares (1999), instead of using a C-Scan (as these specimens are translucent), it is possible to view the damage simply by back-lighting the plates. This gives the approximate damage area, and also a qualitative description of the damage.

2.3 Indentation test

An Instron universal testing machine in Tarbiat Modares University was used to carry out the quasi-static indentation tests on the laminated composite plates. The clamping device and the fixture unsupported span were all the same as high velocity impact tests. As Fig. 2 shows, the indenter nose geometries were all similar to impact test projectiles with the exception that the indenter shank was longer. The dimensions of different nose shapes are shown in Fig. 2. The indenters were located on the apparatus cross-head and perforated the composite plates with the constant cross-head speed of 5 mm/min. the contact force (Mutual force between indenter and sample) is measured by a calibrated load cell which is located at the top of the indenters. The variations of contact force versus dent depth were the outputs of these experiments for different nose shapes. The indentation tests were continued up to the full perforation when the load-displacement curves stabilized.

3. Results and discussion

3.1 Impact test results

As mentioned earlier, the input and output of high velocity impact tests were initial and residual velocity of projectile, respectively. So for each projectile, the residual velocities were obtained for different initial velocities mostly higher than ballistic limit. In total, more than 45 ballistic tests were conducted for different projectile geometries. The results of impact tests, initial velocity, residual velocity and energy absorption (energy absorbed during penetration), are presented in Table 1.

The experimental results are presented in the form of ballistic diagrams, i.e., the curve of residual velocity versus initial velocity. Several analytical models are used to approximate the ballistic curve. Eq. (1) was first proposed by Recht and Ipson (1963).

$$V_R = \alpha(V_I^2 - V_{BL}^2)^{\frac{1}{2}} \quad (1)$$

Where V_R is the residual velocity, V_I is initial velocity, V_{BL} is ballistic limit and α is a curve fitting parameter. Later this equation was modified by Lambert and Jonas (1852) in the form of Eq. (2).

$$V_R = \beta(V_I^P - V_{BL}^P)^{\frac{1}{P}} \quad (2)$$

Where β and P are the curve fitting parameters.

Table 1 Results of ballistic impact tests

Projectile type	Initial velocity (m/s)	Residual velocity (m/s)	Absorbed energy (J)
Flat-ended	156	0 (Partial penetration)	113
Flat-ended	159	13	117
Flat-ended	164	69	103
Flat-ended	166	106 (Deviation)	-----
Flat-ended	172	105	86
Flat-ended	178	126	74
Hemispherical	138	0 (Without penetration)	89
Hemispherical	145	0 (Partial penetration)	98
Hemispherical	157	69	92
Hemispherical	161	83	88
Hemispherical	164	80	95
Conical (90°)	134	0 (Partial penetration)	83
Conical (90°)	139	19	88
Conical (90°)	145	80	68
Conical (90°)	157	85	81
Conical (90°)	165	108	72
Ogival (CRH = 1.5)	141	0	92
Ogival (CRH = 1.5)	144	24	94

Table 1 Continued

Projectile type	Initial velocity (m/s)	Residual velocity (m/s)	Absorbed energy (J)
Ogival (CRH = 1.5)	150	Deviation	-----
Ogival (CRH = 1.5)	153	Deviation	-----
Ogival (CRH = 1.5)	153	83	77
Ogival (CRH = 1.5)	156	62	95
Ogival (CRH = 1.5)	163	98	79
Ogival (CRH = 1.5)	171	107	83
Ogival (CRH = 2.5)	140	89	54
Ogival (CRH = 2.5)	145	85	64
Ogival (CRH = 2.5)	150	0 (ricocheted)	-----
Ogival (CRH = 2.5)	157	97	71
Ogival (CRH = 2.5)	164	19 (ricocheted)	-----
Ogival (CRH = 2.5)	165	119	60
Conical (37°)	120	0 (ricocheted)	67
Conical (37°)	126	0 (passed)	74
Conical (37°)	137	0 (ricocheted)	-----
Conical (37°)	137	49	76
Conical (37°)	145	0 (ricocheted)	-----
Conical (37°)	155	85	78
Conical (37°)	169	125	60

It is shown that this model can estimate the ballistic behavior with a higher precision (Jordan *et al.* 2013). Curve fitting tool of Matlab was used to calculate the values of these parameters for the best fit of experimental data. Ballistic limit, curve fitting parameters and its coefficient of determination for different projectiles have been provided in Table 2. Also the experimental data and their fitted curves are presented into two separate diagrams. Fig. 4(a) shows the experimental data and fitted curves of the flat-ended and the two ogival projectiles. The hemispherical and two conical projectiles are presented in Fig. 4(b). The fitted curves of all six projectiles can be compared in Fig. 4(c).

Table 2 Ballistic limit, curve fit parameters for different projectiles

Projectile	Ballistic limit (m/s)	β	P	r^2
Ogival (CRH = 2.5)	120	1.11	1.90	0.96
Conical (37°)	126	1.51	1.44	0.99
Conical (90°)	136	1.13	2.06	0.92
Ogival (CRH = 1.5)	142	1.23	1.87	0.94
Hemispherical	145	1.05	2.11	0.98
Flat-ended	158	1.98	1.69	0.99

3.2 Indentation test results

In this experiment, the load-displacement diagrams are obtained for different indenters. Three repetitive tests were performed for each indenter to ensure the repeatability of the experiments. The final result of each case is obtained by averaging the results of similar repetitive tests (that are very similar) for each nose shape. Fig. 5(a) shows the load displacement curves for different indenters. In general, the load-displacement curves are formed of five distinct parts, which are identified in Fig. 5(b).

At beginning of the graph, the linear section of AB is located. In this section, a global elastic deformation occurs in composite laminates without any damage or failure. The point B is where the damage starts in the composite. This damage can be matrix crack initiation, delamination or beginning of the indenter penetration. In the BC section, the plate deflection continues nonlinearly and the aforementioned damages slowly spread in the laminate. The linear elastic section is observed in flat-ended and hemispherical indenters. Sharper indenters penetrate into composite plate from beginning of the perforation process so their load-displacement curves are started from point B. Usually, only one of the AB or BC regions is observed in thin laminates. When the laminate thickness increases, both sections AB and BC can be observed simultaneously (Xiao *et al.* 2007). As the deflection increases, at a specific point (point C) a sudden damage occurs in the composite laminate and the contact force shows a small drop, depending on the indenter shape. This point is the starting of shear plug formation in flat-ended indenter while for other indenters, petalling starts at point C. The CD section is usually seen in flat-ended indenters and is related to shear plug ejection in the front layers of composite.

In the DE region, the formed petals expand with at a nearly constant force. The slope of load deformation curve in this area is dependent on the size and angle of the petals. The petal growth becomes slower for indenters with longer nose and the DE region will be elongated. When the indenter shank reaches to composite plate, petal expansion stops and a sudden drop of contact force is observed (EF section). At the end of the perforation process, load-displacement graph becomes nearly horizontal and the only force resisting the indenter motion is the frictional force between indenter shank and composite laminate (point F).

3.3 Perforation mechanisms

3.3.1 Flat-ended perforator

A sample of the perforation of laminate composite by flat-ended projectile and indenter are shown in Fig. 6. In both cases, the perforation mechanism is a combination of shear plug ejection in front layers and petal formation of back layers. The thicknesses of ejected plugs are almost identical and equal to 60% of laminate total thickness. The only difference between high velocity impact and indentation perforation mechanisms is the dissimilarity of formed petals which is due to non-ideal conditions of the experiments. In high velocity perforation, projectile deviates during penetrating into composite laminate, which is due to non-ideal conditions of impact experiment. Possibility of composite non-uniformity at the area of impact, probability of projectile oblique penetration (i.e. not exact perpendicular penetration), possibility of the deviation of projectile impact at the exact target center, non-uniform growth of the petals, etc. are some inevitable factors which contribute to the projectile deviation during perforation. The maximum deviation of the flat-ended projectile is about 12° and is observed in ballistic limit. Perforation conditions are more ideal in indentation test due to the controls which are applied over the testing process such as

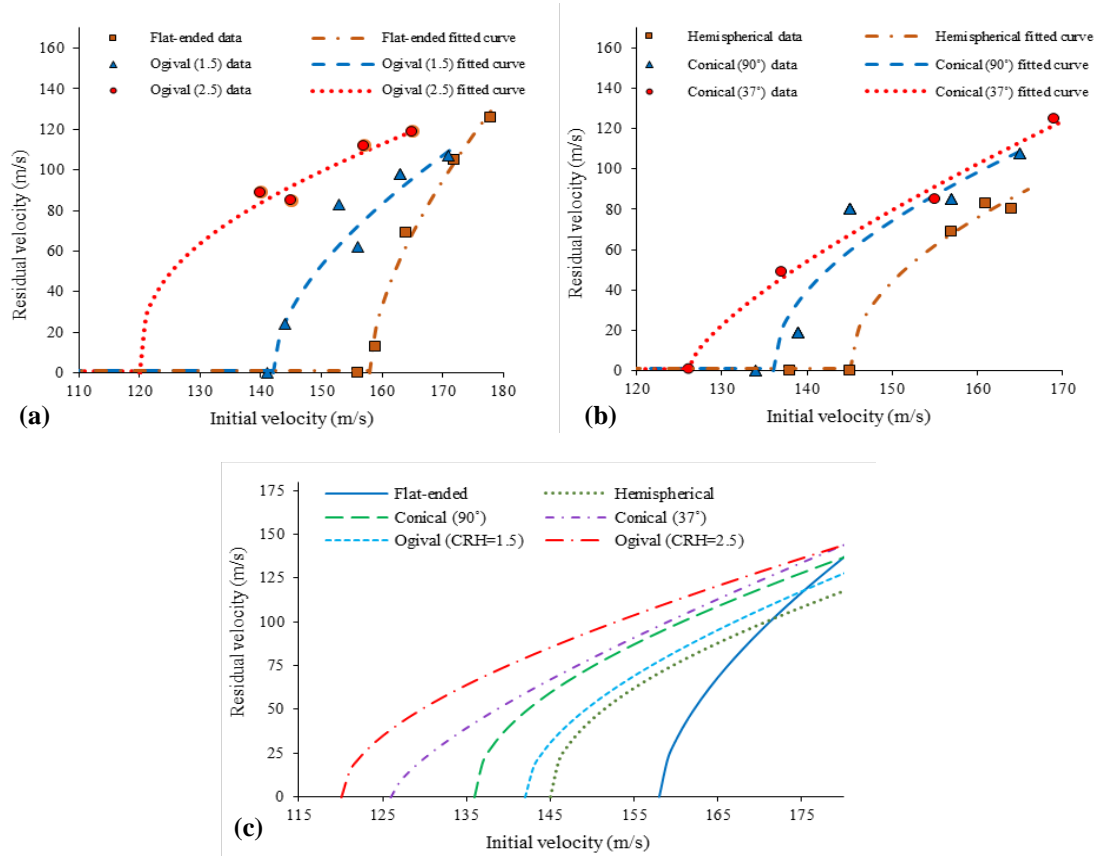


Fig. 4 Experimental data and fitted curves of residual velocity versus initial velocity diagrams in ballistic tests: (a) flat-ended and ogival projectiles; (b) hemispherical and ogival projectiles; (c) ballistic curves of all projectiles

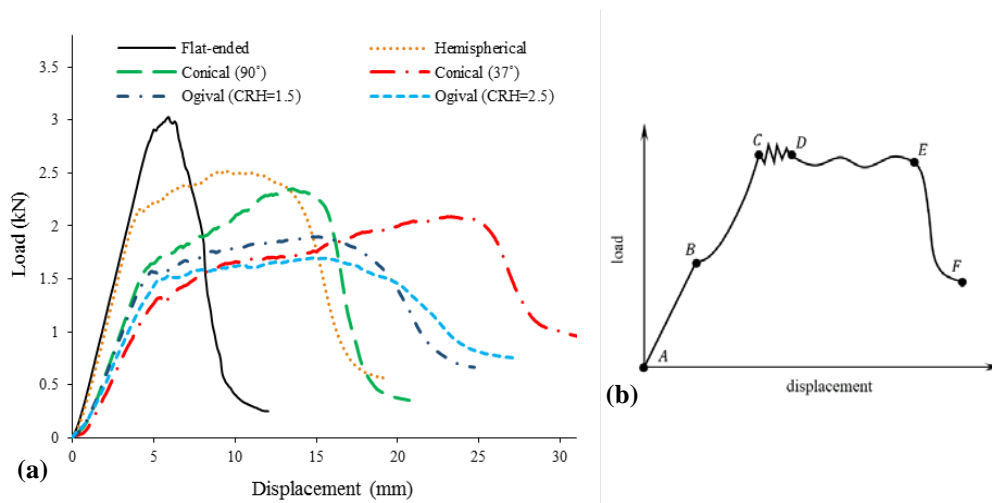


Fig. 5 (a) Load-displacement curves for different indenters; (b) distinct parts of load displacement curve

perpendicular penetration, target center alignment, etc. In ideal conditions, as the indentation test results showed, the flat ended perforator tends to make four similar petals from back layers. In ballistic tests, projectile deviation causes one of the petals to grow more (in deviated direction) than three other petals so in this case, the projectile can perforate with less energy as the deviated flat-ended projectile in Table 1 shows.

3.3.2 Hemispherical perforator

Fig. 7 shows the laminated composite perforation mechanisms against hemispherical perforators in indentation and high velocity ballistic impact tests. Both of the experiments are causing four symmetric petals growth. Deviation of hemispherical projectile in high velocity ballistic test is much less than flat-ended projectile so it shows a desirable similarity to indentation test. The area of formed petals is increased with increasing the initial impact velocity.

3.3.3 Conical perforators

The perforation of glass/epoxy laminate composite by 90° and 37° conical perforators are shown in Figs. 8 and 9. Petal forming is the perforation mechanism in this perforator geometry shape. Due to the low value of projectile deviation, indentation and high velocity impact

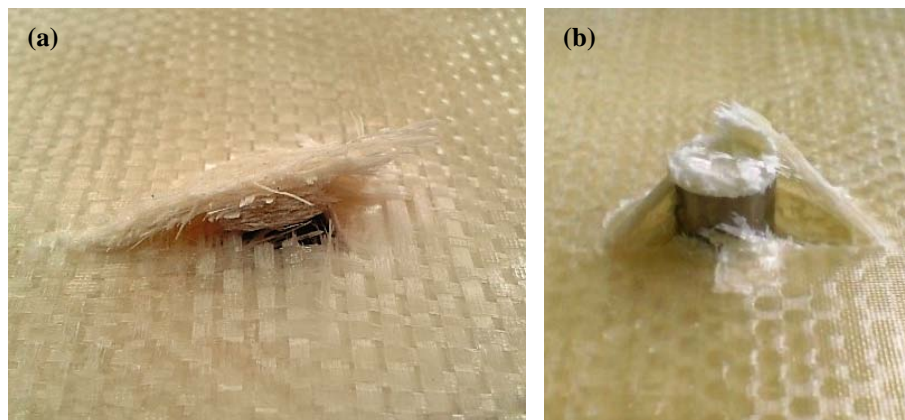


Fig. 6 Perforation mechanism of flat-ended perforator: (a) high velocity impact; (b) quasi-static indentation

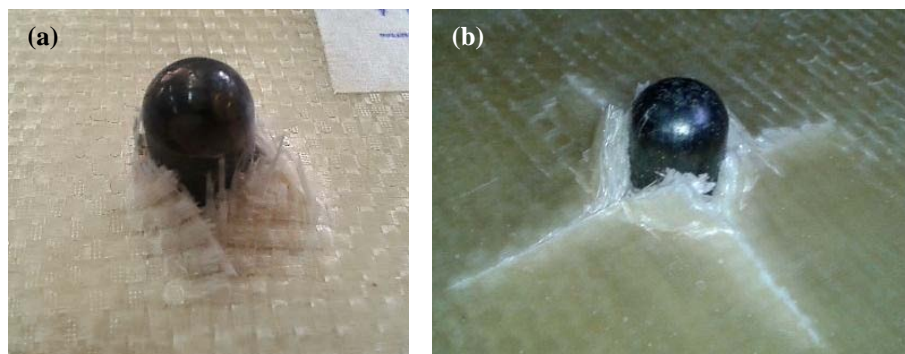


Fig. 7 Perforation mechanism of hemispherical perforator: (a) high velocity impact; (b) quasi-static indentation

experiments behave in a similar way and show four almost identical petals. In this case, the area of formed petals is less than the petals area formed by hemispherical perforator. In this study, two conical perforators (cone angle of 37° and 90°) were investigated. Another phenomenon was observed for projectiles with sharper nose (or in the other hand longer nose). The 37° conical projectile ricochets at velocities close to ballistic limit. A ricochet is when a projectile rebounds off or deviates from the front surface of a target before penetration occurs. The probability of ricochet is dependent on many factors, including projectile shape, material, spin, velocity, angle of incidence and target material. Some conditions such as projectile sharp nose, target flat surface and high target hardness increase the probability of projectile ricochet. Projectile ricochet severely reduces its ballistic performance at velocities close to ballistic limit. With increasing initial impact velocity, the effect of geometry of projectile nose and inhomogeneity of laminate composite is decreases. Therefore, the possibility of ricochet decreases with increasing initial impact velocity.

3.3.4 Ogival perforators

Two ogival perforators with different caliber radius heads were studied in this paper. The CRH of 1.5 and 2.5 were used. Figs. 10 and 11 show the composite perforation mechanisms against 1.5 CRH and 2.5 CRH perforators. Getting the proper results of high velocity experiments for ogival

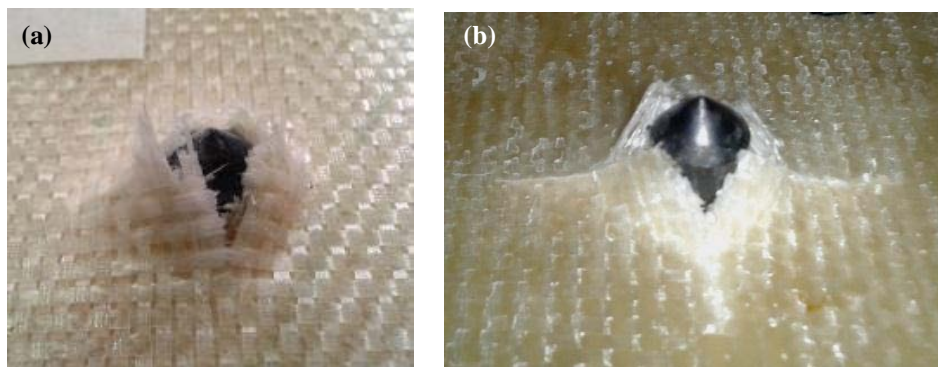


Fig. 8 Perforation mechanism of 90° conical perforator: (a) high velocity impact; (b) quasi-static indentation

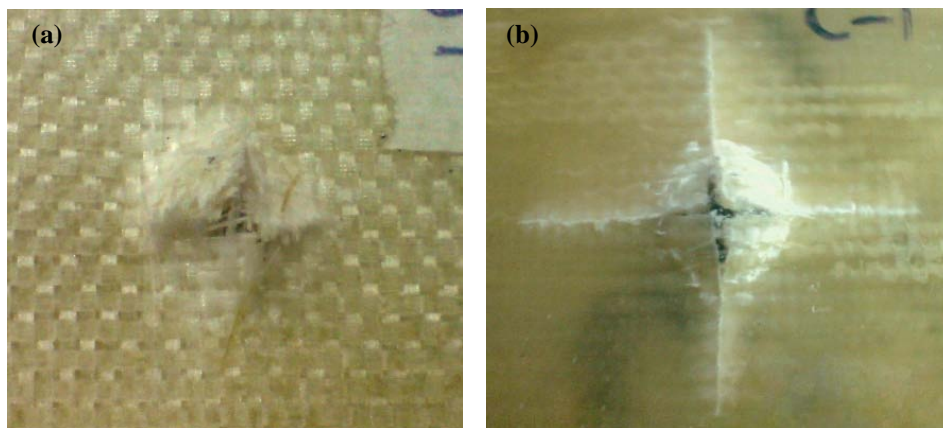


Fig. 9 Perforation mechanism of 37° conical perforator: (a) high velocity impact; (b) quasi-static indentation

projectiles is relatively difficult due to high deviation of 1.5 CRH ogival projectile and high ricochet of 2.5 CRH ogival projectile at velocities close to ballistic limit. Ogival perforators create four symmetric petals in both indentation and high velocity experiments.

In terms of perforation mechanisms of different perforators, there is a great similarity between the results of high velocity ballistic impact experiment and quasi-static indentation test. In flat-ended perforators, the ejected shear plugs are very similar and if ideal impact conditions are satisfied then similar petals will be formed. There is also a desirable similarity in the laminate composite failure modes between high velocity ballistic impact experiment and indentation test for other perforator geometries. Therefore, if perforation mechanisms are of interest, high velocity ballistic impact can be replaced with indentation tests in order to provide the possibility of ballistic failure mode prediction. In this situation, the desirable results can be acquired easier, faster and cheaper for perforation mechanisms of laminated composite.

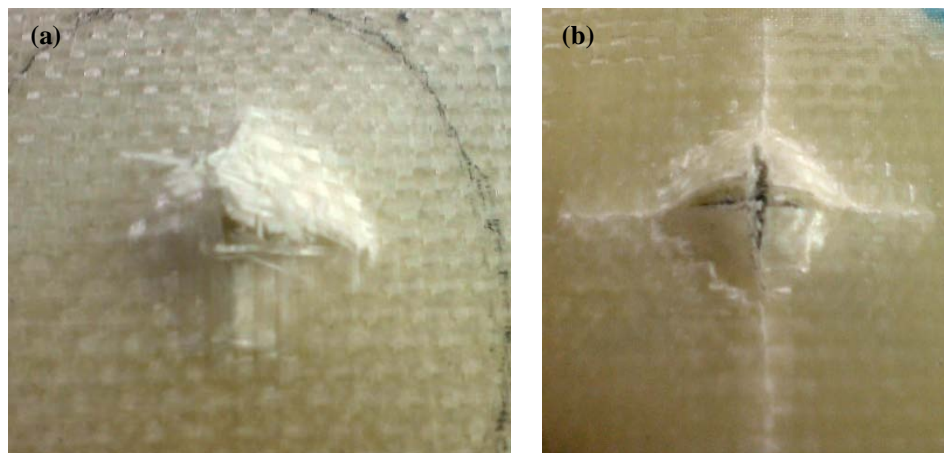


Fig. 10 Perforation mechanism of 1.5 CRH ogival perforator: (a) high impact impact; (b) quasi-static indentation

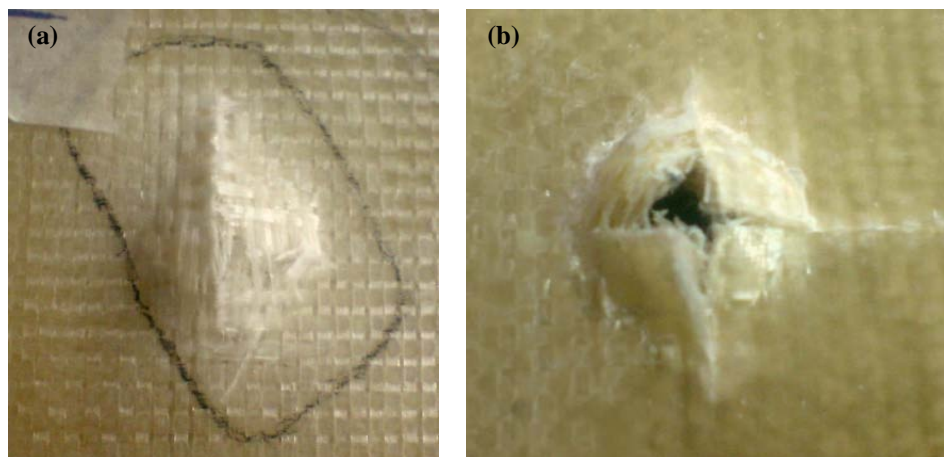


Fig. 11 Perforation mechanism of 2.5 CRH ogival perforator: (a) high impact impact; (b) quasi-static indentation

3.4 Performance of perforators

3.4.1 High velocity impact

In high velocity perforation, the best performance is provided by the projectiles which can perforate the target with the lowest initial velocity. The ballistic curves for the projectiles with different nose shape were presented in Fig. 4(c). As the ballistic curves show, the maximum difference between the performances of different projectiles is observed close to ballistic limit. The minimum velocity required for complete perforation, i.e. ballistic limit, for each projectile are shown in Table 2. As Table 2 shows, the projectiles in high velocity impact, in order of higher performance, are ogival with CRH of 2.5, conical with cone angle of 37° , conical with cone angle of 90° , ogival with CRH of 1.5, hemispherical and flat-ended.

By increasing the initial velocity, the difference between the residual velocities among different shaped projectiles reduces. They offer an almost similar behavior at higher velocities. The flat-ended projectile demonstrates a distinct behavior at higher velocities further than ballistic limit region. Close to ballistic limit region, the flat-ended projectile has the weakest performance, while in high velocities (approximately higher than 180 m/s), it tends to show the performance improvement, relatively. This distinction may be due to the different type of perforation mechanisms created by flat-ended projectile.

Sharper projectiles such as 2.5 CRH ogival projectile and 37° conical projectile have the best performance in ideal impact conditions. If the impact conditions deviate from ideal conditions, then the performance of these kinds of projectiles will strictly decreases due to the ricochet phenomenon.

3.4.2 Quasi-static indentation

Table 3 shows the lowest force necessary for full perforation, namely the peak of load displacement curves, for each indenter. As Table 3 shows, the performance sequence of indenters in quasi-static indentation are ogival with CRH of 2.5, ogival with CRH of 1.5, conical with cone angle of 37° , conical with cone angle of 90° , hemispherical and flat-ended.

Larger global deflection of the laminated composite target in blunt indenters causes that the maximum interaction force increases. Sharper nose shape does not necessarily mean less contact force. E.g., the 37° conical indenter has the sharpest nose but its contact force is more than ogival indenters. Full penetration of the 2.5 CRH ogival indenter into the laminated composite target requires less force, hence this indenter provides the best performance. So it can be concluded that the angle of nose-shank connection is also a significant factor affecting the indenter performance. Tangency of indenter nose to its shank in ogival indenters makes them to penetrate the target with an almost constant force at petal expansion stage (section DE in Fig. 5), while the angled shape of

Table 3 Maximum contact force for different indenters

Order	Indenter	Maximum contact force (N)
6	Ogival CRH = 2.5	1700
5	Ogival CRH = 1.5	1900
4	Conical 37°	2090
3	Conical 90°	2350
2	Hemispherical	2520
1	Flat-ended	3030

nose-shank connection in conical indenters postpones the maximum force to the end of petal expansion stage.

Similar and comparable results are observed for the perforation performance of different shaped perforators in indentation and high velocity ballistic impact experiments. In both experiments, sharper perforators (especially the ogival perforators with CRH of 2.5) provided the best performance and the blunt perforators (especially the flat-ended perforators) are more difficult to penetrate the target in comparison with the other perforators. The only difference in the results of these two experiments is the performance of ogival perforator with CRH of 1.5. This perforator indicated a high performance in indentation tests, while in the high velocity impact experiments, this was not valid. This performance can be due to the conditions encountered in the high velocity ballistic impact experiments. As mentioned before, deviation of 1.5 CRH ogival projectile during perforation from ideal conditions of impact is relatively high. As a result, the ballistic performance of this projectile is severely decreased, while the indentation test conditions are more ideal.

According to the results of high velocity and quasi-static experiments, it can be concluded that the quasi-static indentation test has a qualitative desirable ability to predict the penetration performance of different shaped perforators in high velocity impact. In ideal conditions of experiment, even the results of indentation tests can perfectly predict the performance of perforators. So, in order to compare the performance of different shaped projectiles in composite laminate perforation, the high velocity ballistic impact experiments can be replaced with quasi-static indentation tests.

3.5 Energy absorption

3.5.1 High velocity impact

Fig. 12 shows the graph of the laminated composite absorbed energy versus initial velocity for projectiles with different nose shapes. As Fig. 12 shows, the maximum energy absorptions occur in blunt projectiles. The absorbed energies consistently decrease with increasing the initial velocity for all projectiles. This reduction is due to shortening of perforation time and contact force duration in higher initial velocities. At higher velocities, the global energy absorption decreases and the target damages turn into localized failures. The flat-ended projectile represents the lowest reduction rate of energy absorption due to its distinct perforation mechanism.

3.5.2 Quasi-static indentation

The amount of indenter energy which is absorbed by composite target is calculated as the area under the load-displacement diagrams up to the complete perforation. The diagram of absorbed energy versus the displacement of different indenters is shown in Fig. 13. When the entire process of perforation is considered, sharp indenters (especially 37° conical indenter) require more energy for full perforation, while the minimum energy is absorbed from the flat-ended indenter. Indentation tests are performed with a constant rate, so longer nose of a sharp indenter prolongs the perforation process. For this reason the absorbed energy is increased in 37° conical and ogival indenters. When the absorbed energies for different indenters are compared in an identical displacement (penetration depth), the laminated composite targets absorb more energy from blunt indenters. This can be due to more global elastic deflection in these cases.

The most of the indenter energy is absorbed during the stage of composite damage propagation, i.e., the DE region from Fig. 5(b), in the majority of the indenters. When the perforation mechanism is petal forming, the role of damage spread step is more prominent in energy absorption.

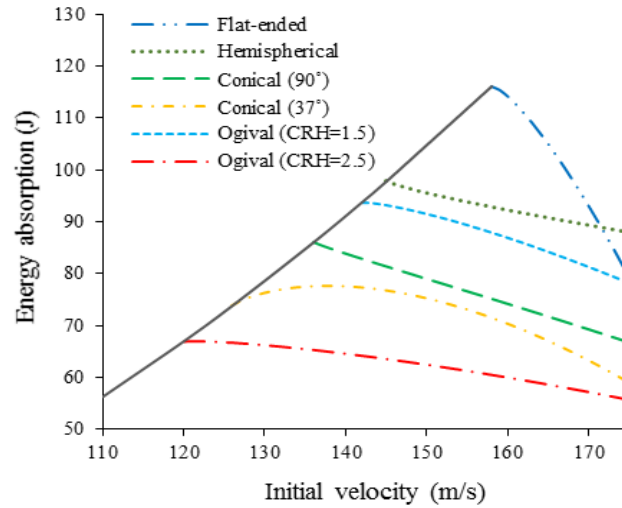


Fig. 12 The laminated composite absorbed energy versus initial velocity for different projectile geometries

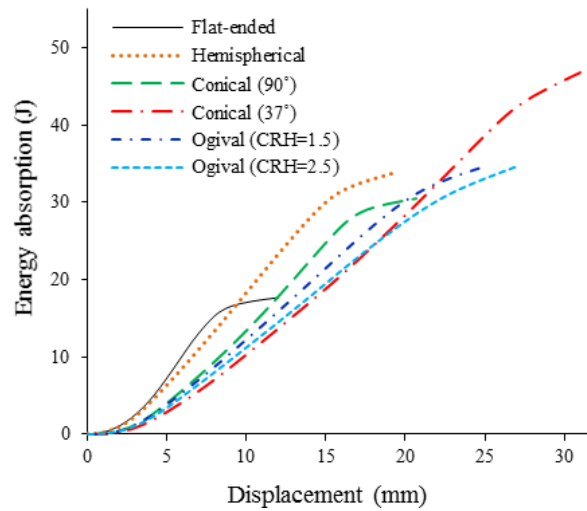


Fig. 13 Absorbed energy versus displacement of different indenters

3.5.3 Dynamic enhancement factor

Dynamic enhancement factor, Φ_p , is a useful measure of impact performance. This factor is defined as the ratio of the dynamic ballistic perforation energy (E_{pd}) to static perforation energy (E_{ps}).

$$\Phi_p = \frac{E_{pd}}{E_{ps}} \quad (3)$$

What this factor reflects is changes in energy absorbing mechanisms due to dynamic effects including inertia (Reid and Zhou 2000). The dynamic perforation energy is calculated by the absorbed energy in ballistic limit for each projectile. Also the static perforation energies are

obtained by quasi-static indentation tests. Table 4 shows the static perforation energy, dynamic perforation energy and dynamic enhancement factor for the different shaped perforators.

Dynamic enhancement factor represents the strain rate effects on the material energy absorption. As Table 4 shows, the value of this factor is consistently more than one, which means that increase of strain rate has a increasing effect on energy absorption of glass/epoxy composite. Whenever the energy absorbing mechanisms are more extensive, the dynamic effects become more influential. The results show that sharp perforators, such as 37° conical and 2.5 CRH ogival perforators, indicate lower values of dynamic enhancement factor due to formation of more localized damages in composite target. The flat-ended perforator represents the maximum dynamic enhancement factor among other perforators. In this state, the extension of damage mechanisms, more deflection, more delamination and occurrence of shear failure increase the dynamic effects.

3.6 Damage area

Delamination area is one of the prevailing forms of failure in laminated composites. In normal laminated composite, there is no reinforcement in the thickness direction. When the laminate is under transverse loading, interlaminar stresses exist in the boundary layer of laminates and plies can be separated. Delamination can also occur during the manufacturing process due to contaminated reinforcing fibers, by insufficient wetting of fibers, or by shrinkage that occurs during the curing of the resin or the subsequent service life of the laminated part (Gordnian *et al.* 2008).

The damaged areas were viewed by back-lighting the plates, instead of using a C-Scan. After taking a picture from plate, the damaged areas were highlighted. Then areas of damaged regions were measured directly by AutoCAD software.

The glass/epoxy laminate composite which is used in this study shows an appropriate interlaminar strength in indentation tests as damage propagated in a small area in these tests. But in high velocity impact tests the damage area is much bigger. So, a limitation of extending quasi-static indentation results to the dynamic perforation tests is the prediction of damage area. Fig. 14 shows examples of composite damage area under quasi-static indentation and high velocity impact tests.

In order to compare the damage area of composite target in high velocity impact experiments for different projectiles, the comparison is performed in experiments with identical initial velocities. The initial impact velocities of 156 m/s and 165 m/s have been both tested for the different projectiles. Fig. 15 shows the target damage area made by different projectiles at these two initial velocities.

Table 4 Dynamic and static perforation energy and dynamic enhancement factor for the different perforators

Perforator	Dynamic energy absorption (J)	Static energy absorption (J)	Dynamic enhancement factor
Conical (37°)	73.8	46.8	1.6
Ogival (CRH = 2.5)	67.0	34.7	1.9
Ogival (CRH = 1.5)	93.8	34.4	2.7
Conical (90°)	86.0	30.4	2.8
Hemispherical	97.8	33.6	2.9
Flat-ended	116.1	17.7	6.6

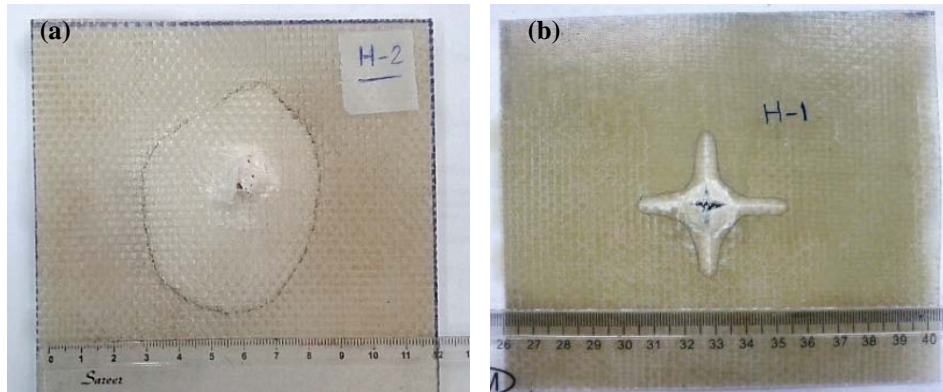


Fig. 14 Damage area for hemispherical perforator: (a) high velocity impact; (b) quasi-static indentation

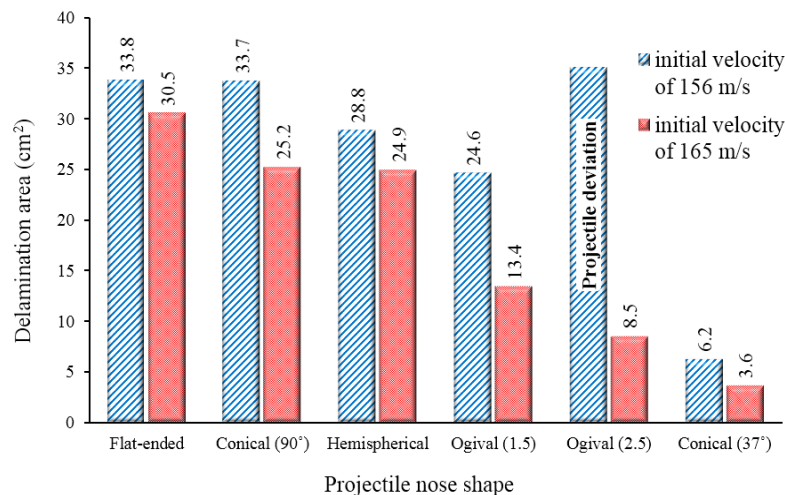


Fig. 15 The size of target damage area made by different projectile geometries at two initial velocities

If large deviation of projectiles does not occur during perforation, the highest damage area will be created by flat-ended projectile. The increase of projectile nose sharpness reduces the damage area, but it is not the only determinant factor of the projectile behavior. However, it should be noted that the joining shape of projectile nose to its shank has a significant effect on projectile performance especially damage area. Abrupt change or sharp edge of this joining increases the composite damage area. This issue is clearly observed in 90° conical and hemispherical projectiles. Although the 90° conical projectile has a sharper edge but its sharp joining edge makes its damage area more than the damage of hemispherical projectile. As a result, there should be an optimal combination of projectile nose angle, nose length and nose-shank joining shape in order to obtain minimum damage area.

Projectile deviation during perforation strongly increases the damage area, as is clearly observed in 37° conical projectile at initial velocity of 156 m/s. The highest damage area is mostly observed in ballistic limit of each projectile. As the initial velocity increases and keeps distance from the ballistic limit, the damage reduces.

Table 5 Friction force in indentation tests

Order	Indenter	Friction force (N)
1	Conical 37°	980
2	Ogival CRH = 2.5	770
3	Ogival CRH = 1.5	680
4	Hemispherical	590
5	Conical 90°	370
6	Flat-ended	270

3.7 Friction force

One of the energy absorption mechanisms in perforation is the friction force. The value of friction force depends on the materials in contact and the normal force between two surfaces. The measurement of projectile force during high velocity impact perforation is very difficult; therefore the friction force effects in high velocity tests were not measured. But in the quasi-static indentation test the indenter force history can be recorded, and the friction force between the indenter and the laminated composite target can be quantified.

In indentation test, when the indenter nose completely passes from the target, the only force resisting the motion of indenter is friction force between indenter shank and the perforated composite. This issue occurs at the end of perforation process, i.e., after point F in Fig. 5, where the load displacement curve is almost horizontal. The friction force is equal to the force that this horizontal section shows. The values of friction force have been provided in Table 5.

Regarding the constant indenter and target materials in all indentation tests, the only factor that changes the friction force of different indenters is the normal force exerted by the petals on the indenter shank. The flat-ended indenter indicates the lowest friction force due to low thickness of formed petals.

4. Conclusions

In this paper, the behavior of laminated composite was experimentally investigated and quasi-static indentation and high velocity impact tests are compared when impacted by different projectile geometries in order to explore the possibility of extending quasi-static indentation test results to high velocity ballistic impact tests in different characteristics such as perforation mechanisms, performance of perforators, energy absorption, friction force, etc. The behavior of glass epoxy laminated composite in quasi-static indentation and high velocity impact tests was investigated using blunt, hemispherical, conical and ogival perforators. Two conical nose perforators with different cone angles and two ogival perforators with different caliber radius head were used to be able to study the effects of perforator nose shape, nose length and joining shape of projectile nose to its shank.

The indentation tests were analyzed using the perforator load displacement curve and the high velocity test data were fitted in the form of ballistic curves using Lambert and Jonas analytical model. The results showed that:

- In high velocity impact tests, the maximum difference between the performances of

different projectiles is observed close to ballistic limit area. The projectiles offer an almost similar behavior at higher impact initial velocities. In higher velocities, the flat-ended projectile relatively tends to show the performance improvement due to its different type of perforation mechanisms.

- In some cases, projectile deviation and ricochet are observed close to ballistic limit due to non-ideal impact conditions. If the impact conditions deviate from ideal conditions, then the performance of sharper projectiles will strictly decreases due to the ricochet phenomenon.
- The quasi-static indentation test has a desirable ability to predict the penetration of different shaped perforators in high velocity impact. In ideal conditions of experiment, even the results of indentation tests can quantitatively predict the performance of perforators. In both experiments, the highest performance occurs for 2.5 CRH projectile and the lowest is related to blunt projectiles.
- Whenever the energy absorbing mechanisms are more extensive, the dynamic effects become more influential.
- The results show that sharp perforators indicate lower values of dynamic enhancement factor due to formation of more localized damages in composite target. Moreover, the flat-ended perforator represents the maximum dynamic enhancement factor among other perforators.
- Damage propagation far more occurred in high velocity impact tests then quasi-static tests. The highest damage area is mostly observed in ballistic limit of each projectile which projectile deviation strongly increases this area. It was showed that there should be an optimal combination of projectile nose angle, nose length and nose-shank joining shape in order to obtain minimum damage area. A limitation of extending quasi-static indentation results to the dynamic perforation tests is the prediction of damage area.

Finally, it can said that a great similarity between the perforation mechanisms of high velocity impact experiment and quasi-static indentation test especially in several characteristics such as failure mechanisms, perforator performance, friction force.

Therefore with this feature, high velocity ballistic impact can be replaced with indentation tests in order to provide the possibility of ballistic failure mode prediction. In this situation, the desirable results can be acquired easier, faster and cheaper for perforation mechanisms of laminated composite.

References

- Al-Hassani, S. and Kaddour, A. (1997), "Strain rate effects on GRP, KRP and CFRP composite laminates", *Key Eng. Mater.*, **141**, 427-452.
- Baucom, J. and Zikry, M. (2003), "Evolution of failure mechanisms in 2D and 3D woven composite systems under quasi-static perforation", *J. Compos. Mater.*, **37**(18), 1651-1674.
- Gordnian, K., Hadavinia, H., Mason, P. and Madenci, E. (2008), "Determination of fracture energy and tensile cohesive strength in Mode I delamination of angle-ply laminated composites", *Compos. Struct.*, **82**(4), 577-586.
- Gama, B.A. and Gillespie Jr., J.W. (2008), "Punch shear based penetration model of ballisti impact of thick-section composites", *Compos. Struct.*, **86**(4), 356-369.
- Icten, B.M., Kiral, B.G. and Deniz, M.E. (2013), "Impactor diameter effect on low velocity impact response of woven glass epoxy composite plates", *Compos. Part B: Eng.*, **50**, 325-332.
- Iremonger, M. and Went, A. (1996), "Ballistic impact of fibre composite armours by fragment-simulating

- projectiles", *Compos. Part A: Appl. Sci. Manuf.*, **27**(7), 575-581.
- Jordan, J.B. and Naito, C.J. (2014), "An experimental investigation of the effect of nose shape on fragments penetrating GFRP", *Int. J. Impact Eng.*, **63**, 63-71.
- Jordan, J.B., Naito, C.J. and Haque, B.Z.G. (2013), "Quasi-static, low-velocity impact and ballistic impact behavior of plain weave E-glass/phenolic composites", *J. Compos. Mater.*, **48**(20), 2505-2516.
- Khodadadi, A., Liaghat, G.H., Akbari, M. and Tahmasebi, M. (2013), "Numerical and experimental analysis of penetration into Kevlar fabrics and investigation of the effective factors on the ballistic performance", *Modares Mech. Eng.*, **13**(12), 124-133.
- Lambert, J. and Jonas, G. (1852), *Towards Standardization in Terminal Ballistics Testing: Velocity Representation. Ballistic Research Laboratories*, Report No. BRL-R; Aberdeen Proving Ground, MA, USA.
- Lee, S.-H., Aono, Y., Noguchi, H. and Cheong, S.-K. (2003), "Damage mechanism of hybrid composites with nonwoven carbon tissue subjected to quasi-static indentation loads", *J. Compos. Mater.*, **37**(4), 333-349.
- Manzella, A., Gama, B. and Gillespie Jr., J. (2011), "Effect of punch and specimen dimensions on the confined compression behavior of S-2 glass/epoxy composites", *Compos. Struct.*, **93**(7), 1726-1737.
- Mines, R., Roach, A. and Jones, N. (1999), "High velocity perforation behaviour of polymer composite laminates", *Int. J. Impact Eng.*, **22**(6), 561-588.
- Mitrevski, T., Marshall, I., Thomson, R., Jones, R. and Whittingham, B. (2005), "The effect of impactor shape on the impact response of composite laminates", *Compos. Struct.*, **67**(2), 139-148.
- Mitrevski, T., Marshall, I., Thomson, R. and Jones, R. (2006), "Low-velocity impacts on preloaded GFRP specimens with various impactor shapes", *Compos. Struct.*, **76**(3), 209-217.
- Muhi, R., Najim, F. and De Moura, M. (2009), "The effect of hybridization on the GFRP behavior under high velocity impact", *Compos. Part B: Eng.*, **40**(8), 798-803.
- Pol, M.H., Liaghat, G. and Hajiarazi, F. (2013), "Effect of nanoclay on ballistic behavior of woven fabric composites: Experimental investigation", *J. Compos. Mater.*, **47**(13), 1563-1573.
- Recht, R. and Ipson, T. (1963), "Ballistic perforation dynamics", *J. Appl. Mech.*, **30**(3), 384-390.
- Reid, S.R. and Zhou, G. (2000), "Impact behaviour of fibre-reinforced composite materials and structures", *CRC Press*.
- Sutherland, L.S. and Soares, C.G. (1999), "Impact test on woven-fabric E-glass/polyester laminates", *Compos. Sci. Technol.*, **59**(9), 1553-1567.
- Ulven, C., Vaidya, U. and Hosur, M. (2003), "Effect of projectile shape during ballistic perforation of VARTM carbon/epoxy composite panels", *Compos. Struct.*, **61**(1), 143-150.
- Wen, H., Reddy, T., Reid, S. and Soden, P. (1997), "Indentation, penetration and perforation of composite laminate and sandwich panels under quasi-static and projectile loading", *Key Eng. Mater.*, **141**, 501-552.
- Xiao, J., Gama, B. and Gillespie Jr., J. (2007), "Progressive damage and delamination in plain weave S-2 glass/SC-15 composites under quasi-static punch-shear loading", *Compos. Struct.*, **78**(2), 182-196.
- Yahaya, R., Sapuan, S.M., Jawaid, M., Leman, Z. and Zainudin, E.S. (2014), "Quasi-static penetration and ballistic properties of kenaf aramid hybrid composites", *Mater. Des.*, **63**(2), 775-782.